Molecular Architecture of the Inner Membrane of Mitochondria from Rat Liver: A Combined Biochemical and Stereological Study

Klaus Schwerzmann, Luis M. Cruz-Orive, Rita Eggman, Alexandra Sänger, and Ewald R. Weibel

Department of Anatomy, University of Berne, 3000 Berne 9, Switzerland

Abstract. The molecular structure of mitochondria and their inner membrane has been studied using a combined approach of stereology and biochemistry. The amount of mitochondrial structures (volume, number, surface area of inner membrane) in a purified preparation of mitochondria from rat liver was estimated by stereological procedures. In the same preparation, the oxidative activity of the respiratory chain with different substrates and the concentration of the redox complexes were measured by biochemical means. By relating the stereological and biochemical data, it was estimated that the individual mitochondrion isolated from rat liver has a volume of 0.27 μm^3, an inner membrane area of 6.5 μm^2, and contains between 2,600 (complex I) and 15,600 (aa_3) redox complexes which produce an electron flow of over 100,000 electrons per second with pyruvate as substrate. The individual redox complexes and the H^+-ATPase together occur at a density of ~7,500/μm^2 and occupy ~40% of the inner membrane area. From the respective densities it was concluded that the mean nearest distance between reaction partners is small enough (70–200 Å) to cause the formation of micro-aggregates. The meaning of these results for the mechanism of mitochondrial energy transduction is discussed.

THE molecular structure of mitochondria and in particular of their inner membrane is of great interest to bioenergetics because most of the enzymes involved in energy transduction are associated with these organelles (7). Many of the energy-transducing enzymes, notably the enzymes of the respiratory chain and the H^+-ATPase, are multisubunit complexes which span the membrane and represent ~80% of the total intrinsic protein mass of this membrane (21). Pictures of freeze-fractured inner membranes show a dense packing with intrinsic proteins (19, 46). How dense the various protein complexes are built into the inner membrane, and how they are distributed along the plane of the membrane is important for the understanding of the mechanism of energy-transducing reactions in mitochondria.

This sort of information is scarce due to the complexity of the mitochondrial ultrastructure and owing to the fact that it is not accessible through biochemical techniques alone. For instance, Gear and Bednarek (15) used a Coulter counter technique to estimate the number and volume of mitochondria in suspension and related these parameters to biochemical data. The Coulter counter method, however, measures only particle size, but cannot give information on the intramitochondrial structures relevant for bioenergetics, such as inner membrane and matrix. In this paper we present an approach which combines biochemical with stereological techniques so as to obtain parameters describing the molecular infrastructure of mitochondria and in particular of the inner membrane. Stereological procedures were applied on electron micrographs of purified preparations of rat liver mitochondria, to estimate mitochondrial number and volume, matrix volume, and surface areas of inner and outer membrane in the suspension. In the same preparation, biochemical parameters were measured to determine the activity of the respiratory chain and the concentration of proteins involved in electron transfer. By relating the respiratory activity and concentration of cytochromes in the aliquots to the amount of the structure present (e.g., mitochondrial volume, matrix volume inner membrane area) novel data on the molecular organization of mitochondria and the inner membrane were derived.

Materials and Methods

Isolation of Mitochondria

Mitochondria were isolated from rat liver (male Wistar rats, 250–350 g, fed ad libitum) according to the procedure by Bustamante et al. (5). The isolation medium (pH 7.4) contained 220 mM mannitol, 70 mM sucrose, 1 mM EGTA, 2 mM Hepes–KOH, and 0.05% fatty acid–free bovine serum albumin (Sigma Chemical Co., St. Louis, MO). The mitochondrial fraction was washed twice in the same medium without the EGTA. To remove microsomal contamination (14), mitochondria were further purified on a Percoll gradient (Pharmacia Fine Chemicals, Uppsala, Sweden). Approximately 1 ml of the mitochondrial suspension (50 mg protein per ml) was mixed with 20 ml of wash medium containing 30% (vol/vol) Percoll and centrifuged for 30 min at 25,000 rpm (Beckman L-65 ultracentrifuge, Type 30 rotor). The mitochondrial layer at the bottom of the tube was easily separated from the upper layer containing mainly microsomal contamination (14). The purified mitochondria were then washed three times with the wash medium to remove all traces of Percoll which was found to inhibit the respiratory chain (not shown).

Biochemical Measurements

Oxygen consumption was measured polarographically at 30°C with a Clark-type O_2-electrode (Yellow Springs Instrument Co., Yellow Springs, OH). The reaction medium (2.24 ml) was identical with the isolation medium supplied with 1 mM $MgCl_2$, 2.5 mM potassium phosphate (pH 7.4), and 2.5 mM of the substrates indicated. With succinate as substrate, 1.1 μM rotenone was included. The oxygen content of the medium was calibrated using submitochondrial particles oxidizing known amounts of NADH.

Cytochrome c oxidation was measured polarographically in presence of ascorbic acid and N,N,N',N'-tetramethyl-1,4-phenylene-diammoniumdichlorid according to Schnaitman and Greenawalt (36). The concentration of cytochromes in the suspension of mitochondria was measured quantitatively with the method of Williams (45). Briefly, difference spectra of mitochondria (5–10 mg protein per ml) were obtained in 50 mM potassium phosphate (pH 7.4) and 0.5 mg of deoxycholate per mg of protein. The concentration of cytochromes b, c_1, c, and aa_3 was calculated from the sodium dithionite reduced versus oxidized spectra using the molar extinction coefficients as given by Schneider et al. (37).

Protein concentrations were determined by a Biuret method (24) with fatty acid-free bovine serum albumin as protein standard.

Electron Microscopic Preparations

Purified mitochondria (5 mg of protein) were diluted into 10 ml of fixation medium (250 mM sucrose, 2 mM Hepes–KOH, 0.5% glutaraldehyde [pH 7.4] 340 mOsm) and fixed for 30 min on ice. Aliquots (0.6 ml) were then transferred into a filtration chamber as described by Baudhuin (3), overlayered with ~2 ml of chilled sodium cacodylate buffer (100 mM, pH 7.4, adjusted to 340 mOsm with sodium chloride), and filtered through millipore filters (pore size 0.22 μm, diameter 13 mm) using a positive air pressure of 0.6 to 1 atm. Filtration was stopped leaving the mitochondrial sediment still covered with buffer. The filter disks were then removed, covered with a similar filter, and clamped into sample holders for further processing. Postfixation with 1% osmium tetroxide, en bloc staining with 3% uranyl acetate, and dehydration with ethanol was done exactly as described previously (4). Prior to embedding, the filters were dissolved in propylene oxide. This resulted in a mitochondrial pellicle which could be embedded as a flat disk.

Stereological Methods

The sampling scheme adopted for stereological analysis is outlined in Fig. 1. The estimation procedures were carried out at three suitably gradated levels of magnification. From each mitochondrial preparation, a simple random sample of five pellicles was chosen. From each pellicle, three small blocks were selected using the vertices of a lattice superimposed randomly on the pellicle (Fig. 1 b). One ultrathin section (50–80 nm, LKB Ultramicrotome) was transferred onto an H-grid for electron microscopy. Sections were always taken approximately vertical, that is, perpendicular to the pellicle faces (Fig. 1 c). Under the electron microscope (Philips EM 300), each section was subsampled at five locations by a carefully designed systematic procedure which eliminates any possible gradients in mitochondrial content within the section (Fig. 1 d). At each location, one micrograph was taken at the three magnifications corresponding to levels I to III (see below). Section thickness was estimated by the fold method of Small (39). Magnifications were assessed with the aid of a carbon grating replica with 1/21,600 cm^{-1} spacing (Ernest F. Fullam Inc., Schenectady, NY). For the analysis, contact prints of 35-mm films were projected onto a screen producing approximately a 10-fold magnification (43).

Level I/Absolute Volume of Pellicle. This was estimated as follows:

$$V(\text{pell}) = \frac{1}{4} \times \pi d^2 \times \bar{\tau} \tag{1}$$

where d is the diameter of the pellicle after embedding ($d = 10$ mm) and $\bar{\tau}$ is the mean pellicle thickness estimated from the low power micrographs (Fig. 2 a) using the aforementioned fact that the sections were approximately perpendicular to the pellicle faces. The range of $\bar{\tau}$ was 8–15 μm.

Level II/Mitochondrial Volume Fraction in the Pellicle. The primary magnification used here was 2,500. The mitochondrial volume fraction in the pellicle was estimated by point counting (43) as follows:

$$\text{est}V_v(\text{mi, pell}) = \Sigma[M_i^{-2} \times \Sigma P_{ij}(\text{mit})]/\Sigma[M_i^{-2} \times \Sigma P_{ij}(\text{pell})] \tag{2}$$

where the summations in i and j are over sections and micrographs, respectively. M_i is the magnification of the i-th section, $P_{ij}(\text{mit})$ is the number of points of the test system (see Fig. 2 b) falling within mitochondrial profiles in the j-th micrograph of the i-th section, and $P_{ij}(\text{pell})$, correspondingly, of the points falling on the entire pellicle material. For a justification of the magnification correction see Cruz-Orive (9). The absolute mitochondrial volume in a pellicle
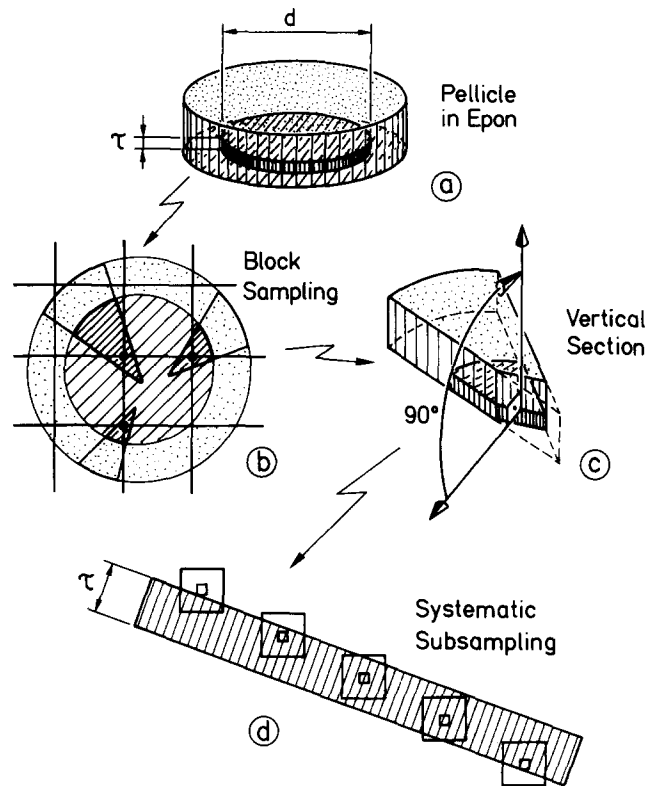
is obtained by multiplying the mitochondrial volume fraction with the absolute volume of the pellicle.

To estimate the mean structural properties of an individual mitochondrion, the mitochondrial number density is also needed. We estimated the latter according to Cruz-Orive (10) as follows:

$$\text{est}N_v(\text{mi, pell}) = N_A/[\bar{T} + \text{est}D \times \cos Z)] \tag{3}$$

where N_A is the observed mean number of mitochondrial profiles per pellicle section area. Profile counts were made in 9 squares per micrograph as shown in Fig. 2 b. An unbiased counting rule was adopted within each square (16). $\bar{T}$ is the mean section thickness, D the mean mitochondrial diameter, and Z the capping angle estimated according to the model of Cruz-Orive (10). To estimate Z, 300–400 mitochondrial profiles were classified into 9 size classes (0–6 mm plus 8 classes with 4 mm class width) using only one square per micrograph (Fig. 2 b). Evidently, the absolute number of mitochondria in a pellicle can then be estimated by multiplying Eq. 3 with the absolute pellicle volume from Eq. 1.

Level III/Surface Area of Inner and Outer Membrane per Mitochondrial Volume. This term, designated also as density of inner or outer membrane, was estimated at a primary magnification of 14,000 by point counting using the test grid shown in Fig. 2 c. For instance, the inner mitochondrial membrane density was estimated as:

$$\text{est}S_v(\text{im, mi}) = (p/l) \times \Sigma[M_i^{-1} \times \Sigma I_{ij}(\text{im})]/\Sigma[M_i^{-2} \times \Sigma P_{ij}(\text{mit})] \tag{4}$$

where the summations in i and j are over sections and micrographs, respectively, p/l is the number of test points per unit length of test line in the test system, I_{ij} (im) the number of intersection points between the inner membrane and the test lines for the j-th micrograph of the i-th section, and $P_{ij}(\text{mit})$ the number of test points falling within mitochondrial profiles. The surface density of the
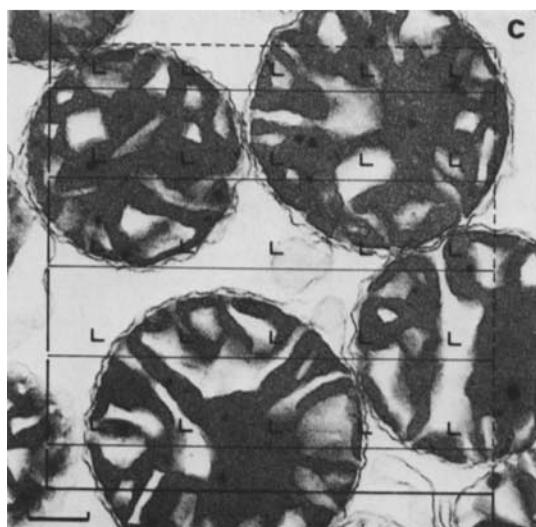

Figure 1. Diagrammatic illustration of the stereological sampling design adopted in this paper for estimating the surface area of inner membrane in isolated mitochondria. (*a*) Pellicle containing purified mitochondria, here represented by a small disk of thickness τ inside a cylindrical Epon block. (*b*) Systematic sampling of small blocks from the pellicle. The lattice has a random position relative to the pellicle. (*c*) From each block a vertical ultrathin section was cut for electron microscopy. (*d*) Systematic subsampling of quadrats (at two different magnifications) from a given vertical section.

outer membrane was estimated accordingly. The absolute membrane areas in a pellicle were obtained by multiplying the respective surface densities with the absolute mitochondrial volume.

Results

As an example, Table I lists the mean stereological data obtained from five pellicles of a mitochondrial preparation. Since mitochondria sediment quantitatively on the filter (3) and the preparation is virtually free of nonmitochondrial material (Fig. 2 a), stereological data could be referred directly to the mass of protein in the pellicle. These values averaged over three preparations of either condensed or orthodox mitochondria (18) are given in Table II. As expected, volume and outer surface area were almost identical for mitochondria fixed in either conformational state. The surface area of inner membrane, however, was found to be lower in orthodox mitochondria. This observation is likely to be an artifact, as lower contrast and resolution of cristae in orthodox mitochondria result in an underestimation of the surface density. Therefore, only the structural data derived from condensed mitochondria were used in further calculations.

Similarly, biochemical measurements done on each mitochondrial preparation were related to the stereological data. For instance, mitochondrial oxygen consumption, normally expressed as activity per mg of protein, could be referred to the amount of relevant structures present, i.e. mitochondrial volume and area inner membrane (Table III). Such volume-specific activities are needed to assess the oxidative capacity of a tissue under different metabolic conditions when the total mitochondrial content can be measured only stereologically (44). On the other hand, a molecular term describing the maximal electron flow per unit membrane area was obtained from the respiratory rates with various substrates and the inner membrane area (Table III). This figure corresponds to the maximal number of electron turnovers in a unit area inner membrane with a given substrate, or, considering the electrons as diffusing species, to the maximal number of electrons diffusing through a unit area of inner membrane in 1 s. As the electron flow density depends not on the activity of single redox complexes alone, but also on the structural organization of the respiratory chain, it could be a useful parameter to characterize the respiratory chain of mitochondria from different sources.

An important parameter describing the structural organization of the redox complexes in the inner membrane is their density which was determined from the concentration of cytochromes and the total inner membrane area in the suspension (Table IV). The approximate numerical densities ranged from 400 complexes I per μm^2 to more than 2,500 cytochrome oxidases per μm^2, corresponding to one complex I per 2,500 nm^2 and one cytochrome oxidase per 400 nm^2,
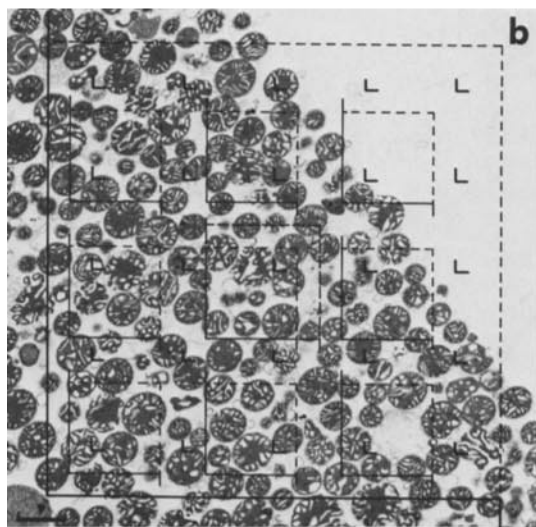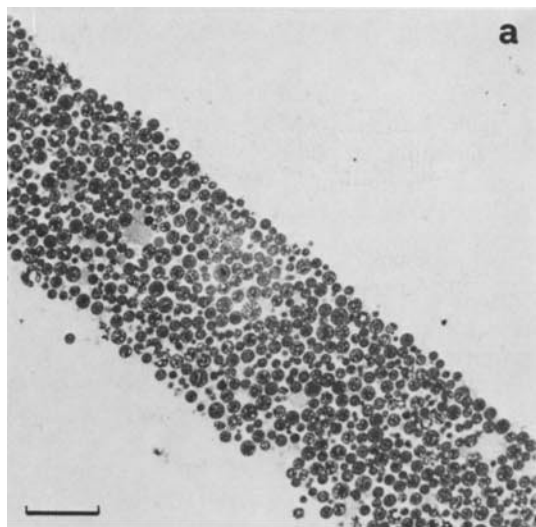
Figure 2. (a) Low magnification quadrat (Level I) from a vertical section of a pellicle, used to estimate mean pellicle thickness and thereby its total volume. Bar, 4 μm. (b) Intermediate magnification quadrat (Level II) used to estimate the volume and number of mitochondria in the pellicle. The volume density was estimated using the 25 test points shown. To estimate mean individual size and number of mitochondria, the nine subquadrats shown were used to count mitochondrial profiles. The necessary sizing of profiles into classes was made from a smaller sample obtained via the central, larger sub-quadrat. The continuous lines represent exclusion edges (16). Bar, 1 μm. (c) Higher magnification quadrat (Level III) with a coherent test system superimposed on it, used to estimate the surface area of inner membrane per unit volume of mitochondria in an efficient way. Bar, 0.2 μm.

respectively. The numerical density of all respiratory complexes including cytochrome c and the H^+-ATPase amounted to over 10,000 per μm^2. Based on published molecular data and assuming a cylindrical shape of these proteins in the membrane, it was estimated that the fraction of inner membrane area covered by the respiratory chain and the H^+-ATPase may be as high as 40% (Table IV).

From the respective densities, the mean minimal distance which protein complexes have to diffuse in order to collide with a reaction partner (35) can be estimated. Such an estimate, the mean nearest-neighbor distance (26) was calculated for the various reaction partners of the respiratory chain and for the three major proton pumps involved in oxidative phosphorylation (Table V). This approximation is applicable

for particles following a Poisson-type random distribution (26), a condition which seems to be met as judged from the particle distribution pattern in freeze-fractured inner membranes (46). Obviously, the mean nearest-neighbor distance depends strongly on the effective density. It was therefore calculated for the two extreme cases of all complexes either in monomeric or dimeric form, with exception of the H^+-ATPase which is known to exist as monomer only (7). It is seen from Table V that the state of aggregation has a big influence on the distance between reaction partners when their numerical density is low. The actual distance, that is the distance from surface to surface, will also depend on the shapes and dimensions of the proteins considered.

Finally, the ultrastructural and functional data were estimated for an individual mitochondrion as it may exist in the suspension (Table VI). Note, however, that the features listed in Table VI may not be representative of mitochondria in situ, as no care was taken to get a representative sample of the whole mitochondrial population of the liver (4).

Discussion

Methodology

In this study we used stereological techniques to quantitate ultrastructural features of isolated mitochondria. This method gives consistent results as is shown by a comparison of our data with those obtained previously by Baudhuin (3) or Bolender et al. (4). Mean mitochondrial volume as well as surface density of inner membranes were very similar to the figures reported here.

In addition, the validity of the stereological data can be checked by comparison with the corresponding data estimated by other methods. For instance, the mitochondrial number and volume per milligram of protein reported by Gear and Bednarek (15) obtained by direct counting and sizing of

Table I. Stereological Data of a Mitochondrial Pellicle Preparation

Parameter	Estimate	
Pellicle thickness	12.5	(0.7) μm
Pellicle volume, V(pell)	0.98	(0.06) mm³
Mitochondrial volume density, V_V(mi, pell)	0.64	(0.02)
Surface density of		
outer membrane, S_V(om, mi)	67,700	(1,000) cm⁻¹
inner membrane, S_V(im, mi)	218,300	(2,800) cm⁻¹
Mitochondrial number density, N_V(mi, pell)	2.52 × 10⁹ mm⁻³	
Total mitochondrial volume, V(mi)	0.66	(0.05) mm³
Total outer membrane area, S(om)	44.9	(3.3) cm²
Total inner membrane area, S(im)	145.2	(11.8) cm²
Total number of mitochondria N(mi, pell)	2.47 × 10⁹	

Each figure is the mean of five pellicles of the same mitochondrial preparation (0.24 mg of protein per pellicle). SEM is indicated in parentheses.

Table II. Structural Parameters of Condensed and Orthodox Mitochondria Related to the Protein Mass Sedimented in the Pellicle

	Condensed*	Orthodox*
Total volume ($\mu l/mg\ protein$)	2.5 (0.3)	2.6 (0.2)
Matrix volume ($\mu l/mg\ protein$)	1.6 (0.2)	—
Outer membrane ($cm^2/mg\ protein$)	155.3 (31.9)	182.4 (8.5)
Inner membrane ($cm^2/mg\ protein$)	520.6 (82.1)	335.8 (30.4)
Number per mg protein	8.7 × 10⁹ (2.5 × 10⁹)	7.0 × 10⁹ (0.7 × 10⁹)

Figures are the means obtained from three mitochondrial preparations. SEM is indicated in parentheses.

* Condensed and orthodox refer to the terminology introduced by Hackenbrock (18). Condensed mitochondria were obtained exactly as described in Methods and Materials, whereas orthodox mitochondria were obtained by prior incubation (10 min, 30°C) of mitochondria in isolation buffer containing 5 mM succinate before fixation.

Table III. Maximal Oxygen Consumption Per Mitochondrial Volume and Inner Membrane Area and Maximal Electron Flow in the Mitochondrial Inner Membrane

Substrates	Maximal O₂-consumption			Maximal electron flow in inner membrane
	per protein mass	per mito. volume	per inner membrane	
	ngatoms/min per mg	ml/min per cm³	ngatoms/min per cm²	e⁻/s per μm^2
Pyruvate + malate	100.2 (32.1)	0.48 (0.21)	0.18 (0.05)	35.9 × 10³
Glutamate	125.6 (17.6)	0.56 (0.11)	0.23 (0.03)	45.0 × 10³
Succinate	350.8 (87.5)	1.72 (0.34)	0.63 (0.10)	125.4 × 10³
Ascorbate + cyt c	656.0*	3.40*	1.24*	249.5 × 10³*

Maximal oxygen consumption was measured in presence of 1.5 μM of an uncoupler, p-trifluoromethoxycarbonyl cyanide phenylhydrazone. Each figure is the mean obtained from three mitochondrial preparations. SEM is indicated in parentheses.

* Mean of two preparations.

mitochondrial particles in suspension were only slightly higher than those in Table II. Measurements for the water-accessible matrix space based on the differential distribution of radioactive tracers also range from 0.8–1.6 μl/mg of protein (20, 40). A figure for the inner membrane area in heart mitochondria is given in a short communication which unfortunately does not reveal the method by which the estimate was obtained (27). Taking into account the higher surface density of cardiac mitochondria (32), the figure of 520 cm^2 of inner membrane per mg of protein in liver seems comparable to the 2,000 cm^2 for heart mitochondria (27).

The stereological data presented here are likely to be more reliable because the sampling design we used avoids bias for particular types of mitochondria (8). In contrast, Coulter counting (15) and light microscopy, the method probably used in reference 27, are heavily biased for larger mitochondria due to the small particle size which is within the limits of resolution of the instrument. Similarly, the determination of the matrix volume with radioactive tracers tends to overestimate the true volume because of the presence of leaky or damaged mitochondria (20).

Possible artifacts in the stereological results would mainly stem from the treatment of the mitochondrial fractions for

Table IV. Density of Energy-transducing Complexes in the Inner Mitochondrial Membrane and Fraction of Inner Membrane Area Covered by Them

Component	Concentration measured	Density in membrane	Approx. Size*	Fraction of inner membrane
	nmol/mg prot.	*N/μm^2*	*Å*	*%*
complex I	0.037[‡]	428	80 [11]	2.2
complex II	0.074[‡]	856	14 [11]	0.1
bc_1-complex	0.078 (0.008)	901 (192)	50 [28]	7.1
cytochrome c	0.236 (0.020)	2753 (226)	20 [41]	0.9
aa_3-complex	0.222 (0.010)	2607 (380)	44 [6]	15.9
$F_1 \cdot F_0$-ATPase	0.222[‡]	2568	90 [2]	16.3

Figures are the means of three preparations. SEM is indicated in parentheses.
* Approximate cylindrical diameter of the monomeric complex as reported in the literature. Brackets denote references.
[‡] Concentration estimated according to references 7 and 22, based on stoichiometries of 0.17 complex I, 0.34 complex II, and 1 $F_1 \cdot F_0$-ATPase, respectively, per 1 aa_3-complex.

Table V. Mean Nearest-Neighbor Distance Between Components of the Mitochondrial Energy-transducing System in the Inner Membrane

Components	Mean nearest neighbor distance	
	All monomeric	All dimeric
	Å	*Å*
complex I–complex II	140	197
complex II–bc_1-complex	119	168
bc_1 complex–cytochrome c	83	117
cytochrome c–aa_3-complex	68	96
bc_1-complex–aa_3-complex	84	119
bc_1-complex–$F_1 \cdot F_0$-ATPase	85	91
aa_3-complex–$F_1 \cdot F_0$-ATPase	70	80

The mean nearest-neighbor distance is calculated from the respective densities according to the formula $0.5 \times (d_1 + d_2)^{-1/2}$ by Keandall and Moran (26), for the two cases of either only monomeric or only dimeric complexes. The $F_1 \cdot F_0$-ATPase is assumed to exist as monomer only (7).

Table VI. Structural and Functional Characteristics of the Average Isolated Mitochondrion

Parameter	Estimate
Diameter (μm)	0.76
Volume (μm^3)	0.27
Outer membrane area (μm^2)	1.93
Inner membrane area (μm^2)	6.47
Protein content (g)	1.1×10^{-13}
Number of molecules of	
complex I	2,679
complex II	5,538
bc_1-complex	5,474
cytochrome c	16,577
aa_3-complex	15,656
$F_1 \cdot F_0$-ATPase	15,656
Maximal O_2-consumption with succinate as substrate (mol/min)	20.2×10^{-18}
ATP-production with succinate as substrate (mol/min)	42.3×10^{-18}

Calculated from Tables II–IV based on 8.7×10^9 mitochondria per mg of protein. ATP-production is determined from the state 3 O_2-consumption and a P/O ratio of 1.6.

electron microscopy, e.g., fixation, dehydration, embedding, sectioning (43). Although the influence of such factors is difficult to assess, there is sufficient evidence that mitochondrial structures are well preserved throughout these steps (32). The problem with underestimating the inner membrane area was overcome by using mitochondria in their condensed form (18) in which cristae are large and of high contrast. We are therefore confident that the stereological estimates reflect the real structural dimensions of mitochondria in suspension. However, due to the isolation procedures, the functional and structural characteristics are not necessarily representative of the single mitochondrion within the hepatic tissue (3, 4) and may change significantly when using different isolation procedures as was demonstrated by Bolender et al. (4).

Mitochondrial Ultrastructure and Bioenergetic Functions

The aim of the study was to improve present knowledge of the functional and molecular features of the average isolated mitochondrion as an energy-transducing unit, and to derive parameters of the molecular architecture of the inner mitochondrial membrane relevant for energy transduction. In this respect, some of the observations merit further discussion.

It was shown in the work of Gear and Bednarek (15) that the average isolated mitochondrion has a small volume but a high content of cytochromes, a finding that is confirmed and extended in this study. The features of an average mitochondrion listed in Table VI, which includes also functional data, point to the extraordinary relationship between mitochondrial volume, inner membrane area, number of respiratory complexes, and respiratory capacity. According to the basic principles of chemiosmosis (29), electron flow through the respiratory chain is coupled to the translocation of protons from the matrix side of the inner membrane to the outer side. This creates a protonic potential which drives the energy-requiring processes in the mitochondrion. If one assumes an $H^+/2e^-$ ratio of 12 (1, 34) and takes the average matrix volume of 2×10^{-16} l (Table VI), the transfer of one pair of electrons from NADH to O_2 through the respiratory chain would be

sufficient to cause a significant drop in internal free protons and, consequently, a dramatic rise of the protonic potential (30). Nevertheless, high rates of over 10^5 electrons per second and mitochondrion can be observed even with coupled respiration (Table III). This discrepancy demonstrates clearly the nature of the coupling mechanism in oxidative phosphorylation as these high rates of electron transfer cannot be explained by a high pH buffering capacity of the matrix alone, but also require a concomitant high back-flow of protons (30). In addition, it presents evidence that the rate of oxidative phosphorylation is not limited by the activity of any of the electron transfer reactions, but rather by the total back-flow of protons through the H^+-ATPase.

A second interesting aspect is the high density of proteins in the inner membrane. It is well known that its integral proteins represent some 40% of the total membrane mass and cover up to 50% of the total membrane area (17, 19, 21, 42), but these figures give no indication on the density of particular proteins. We have been able to determine the density of each of the five multi-subunit complexes of oxidative phosphorylation which together occur at a density of over $7,000/\mu m^2$, corresponding to 1 in 150 nm^2. This is in line with the value reported by Klingenberg (27) of 1 cytochrome a per 500 nm^2. Since these enzyme complexes contain up to 26 single polypeptides of which many are considered to be intrinsic (7), the occupation of the inner mitochondrial membrane with proteins exceeds that of other intracellular membranes by far. In comparison, the membranes of the Golgi apparatus or the endoplasmic reticulum contain only some 30,000 single polypeptides per μm^2 (33).

The dense packing of the inner membrane with proteins is also evident from the estimates of area taken up by the proteins of energy transduction. Although the actual dimensions of those parts of the proteins which extend into the lipid bilayer, as well as their shape, can only be guessed from known molecular data, the estimate of 40% obtained here compares well with other published data (19, 42). Definitely, in other membranes the area occupied with proteins is much lower, with only 10% in the plasma membrane of erythrocytes (13), and 24% in a protein-rich membrane, the retinal rod outer disk membrane (12).

Finally, the mean nearest-neighbor distance, a probabilistic value (26), suggests that at least some of the energy-transducing proteins may be in close contact with one another. The underlying assumption of a Poisson-type random distribution seems to be realistic for most naturally occurring distribution patterns (26). The mean nearest-distance (center-center) between reaction partners ranges from 200 Å between dimeric complexes I and II, to only 80 Å between bc$_1$-complex and cytochrome oxidase with each in monomeric form. The actual mean distance (surface-surface) between some complexes may therefore be well within the range of intramolecular forces which could cause aggregation of complexes (42). This conclusion is supported by recent measurements of rotational diffusion of cytochrome oxidase (25), ADP/ATP-translocator (31), and cytochrome c (23) in native inner membranes, indicating the presence of immobilized populations. In addition, freeze-fractured inner membranes rapidly frozen by the propane–jet method show dispersed proteins as well as micro-aggregates (25). Whether such molecular aggregates have a role in regulating oxidative phosphorylation remains to be seen (23, 25, 31). However, the existence of aggregates, the

dense packing with proteins and the concommittant narrow spacing indicate that there may be structural restraints which limit the free lateral and rotational diffusion of protein complexes in the inner mitochondrial membrane (17, 19).

To summarize, the paper shows that the combination of stereology and biochemistry makes a valuable tool to describe the molecular architecture of biological structures (38), in particular of membranes. The information derived thereof can then be used to critically assess the mechanism of biochemical reactions associated with the biological structure.

References

1. Alexandre, A., and A. L. Lehninger. 1979. Stoichiometry of H^+ translocation coupled to electron flow from succinate to cytochrome c in mitochondria. *J. Biol. Chem.* 254:11555–11560.
2. Amzel, L. M., M. McKinney, P. Narayan, and P. L. Pedersen. 1982. Structure of the mitochondrial F1-ATPase at 9-Å resolution. *Proc. Natl. Acad. Sci. USA.* 79:5852–5856.
3. Baudhuin, P. 1974. Morphometry of subcellular fractions. *Methods Enzymol.* 32:3–20.
4. Bolender, R. P., D. Paumgartner, G. Losa, D. Muellener, and E. R. Weibel. 1978. Integrated stereological and biochemical studies on hepatic membranes. I. Membrane recoveries in subcellular fractions. *J. Cell Biol.* 77:565–583.
5. Bustamante, E., J. W. Soper, and P. L. Pedersen. 1977. A high-yield preparative method for the isolation of rat liver mitochondria. *Anal. Biochem.* 80:401–408.
6. Capaldi, R. A., F. Malatesta, and V. M. Darley-Usmar. 1983. The structure of cytochrome oxidase. *Biochim. Biophys. Acta.* 726:135–148.
7. Capaldi, R. A. 1982. Arrangements of proteins in the mitochondrial inner membrane. *Biochim. Biophys. Acta.* 694:201–306.
8. Cruz-Orive, L. M., and E. R. Weibel. 1981. Sampling designs for stereology. *J. Microscopy.* 122:235–257.
9. Cruz-Orive, L. M. 1982. The use of quadrats and test systems in stereology, including magnification corrections. *J. Microscopy.* 125:89–102.
10. Cruz-Orive, L. M. 1983. Distribution-free estimation of sphere size distributions from slabs showing overprojection and truncation, with a review of previous methods. *J. Microscopy.* 131:265–290.
11. DePierre, J. W., and L. Ernster. 1977. Enzyme topology of intracellular membranes. *Annu. Rev. Biochem.* 46:201–261.
12. Dratz, E. A., and R. A. Hargreave. 1983. The structure of rhodopsin and the rod outer segment disc membrane. *Trends Biochem. Sci.* 8:128–131.
13. Engleman, D. M. 1969. Surface area per lipid molecule in the intact membrane of the human red cell. *Nature (Lond.).* 223:1279–1280.
14. Gazzotti, P., M. Flura, and M. Gloor. 1985. The association of calmodulin with subcellular fractions isolated from rat liver. *Biochem. Biophys. Res. Commun.* 127:358–365.
15. Gear, A. R. L., and J. M. Bednarek. 1972. Direct counting and sizing of mitochondria in solution. *J. Cell Biol.* 54:325–345.
16. Gundersen, H. J. G. 1977. Notes on the estimation of the numerical density of arbitrary profiles: the edge effect. *J. Microscopy.* 111:219–223.
17. Gupte, S., E-S. Wu, L. Hoechli, M. Hoechli, K. Jacobson, A. E. Sowers, and C. R. Hackenbrock. 1984. Relationship between lateral diffusion, collision frequency, and electron transfer of mitochondrial inner membrane oxidation-reduction components. *Proc. Natl. Acad. Sci. USA.* 81:2606–2610.
18. Hackenbrock, C. R. 1966. Ultrastructural bases for metabolically linked mechanical activity in mitochondria. I. Reversible ultrastructural changes with change in metabolic state in isolated rat liver mitochondria. *J. Cell Biol.* 30:269–297.
19. Hackenbrock, C. R. 1981. Lateral diffusion and electron transfer in the inner mitochondrial membrane. *Trends Biochem. Sci.* 6:151–154.
20. Halestrap, A. P., and P. T. Quinlan. 1983. The intramitochondrial volume measured using sucrose as an extramitochondrial marker overestimates the true matrix volume determined with mannitol. *Biochem. J.* 214:387–393.
21. Harmon, H. J., J. P. Hall, and F. L. Crane. 1974. Structure of mitochondrial cristae membranes. *Biochim. Biophys. Acta.* 344:119–155.

22. Hatefi, Y., and Y. Galante. 1978. Organization of the mitochondrial respiratory chain. *In* Energy Conservation in Biological Membranes. G. Schaefer and M. Klingenberg, editors. Springer-Verlag, Berlin, Heidelberg, New York. 19–30.

23. Hochman, J. H., M. Schindler, J. G. Lee, and S. Ferguson-Miller. 1982. Lateral mobility of cytochrome c on intact mitochondrial membranes as determined by fluorescence redistribution after photobleaching. *Proc. Natl. Acad. Sci. USA.* 79:6866–6870.

24. Jacobs, E. E., M. Jacob, D. R. Sanadi, and L. B. Bradley. 1956. Uncoupling of oxidative phosphorylation by cadmium ions. *J. Biol. Chem.* 223:147–156.

25. Kawato, S., C. Lehner, M. Mueller, and R. J. Cherry. 1982. Protein-protein interactions of cytochrome oxidase in inner mitochondrial membranes. The effect of liposome fusion on protein rotational mobility. *J. Biol. Chem.* 257:6470–6474.

26. Kendall, M. G., and P. A. P. Moran. 1963. Geometrical Probability. Charles Griffin, London.

27. Klingenberg, M. 1967. The density of occupation of the mitochondrial membrane by respiratory chain components. *In* Mitochondrial Structure and Compartmentation. E. Quagliariello, S. Papa, E. C. Slater, and J. M. Tager, editors. Adriatica Editrice, Bari. 124–126.

28. Leonard, K., P. Wingfield, T. Arad, and H. Weiss. 1981. Three-dimensional structure of ubiquinol: cytochrome c reductase form neurospora mitochondria determined by electron microscopy of membrane crystals. *J. Mol. Biol.* 149:259–274.

29. Mitchell, P. 1968. Chemiosmotic coupling and energy transduction. Research Institute, Bodmin.

30. Mitchell, P. 1977. A commentary on alternative hypotheses on protonic coupling in the membrane systems catalysing oxidative and photosynthetic phosphorylation. *FEBS (Fed. Eur. Biochem. Soc.) Lett.* 78:1–20.

31. Mueller, M., J. J. R. Krebs, R. J. Cherry, and S. Kawato. 1984. Rotational diffusion of the ADP/ADP translocator in the inner membrane of mitochondria and in proteoliposomes. *J. Biol. Chem.* 259:3037–3043.

32. Munn, E. A. 1974. The Structure of Mitochondria. Academic Press, Ltd. London.

33. Quinn, P., G. Griffiths, and G. Warren. 1984. Density of newly synthesized plasma membrane proteins in intracellular membranes. II. Biochemical studies. *J. Cell. Biol.* 98:2142–2147.

34. Reynafarje, B., and A. L. Lehninger. 1978. The K+/site and H+/site stoichiometry of mitochondrial electron transport. *J. Biol. Chem.* 253:6331–6334.

35. Saffman, P. G., and M. Delbruck. 1975. Brownian motion in biological membranes. *Proc. Natl. Acad. Sci. USA.* 72:3111–3115.

36. Schnaitman, C., and J. W. Greenawalt. 1968. Enzymatic properties of the inner and outer membranes of rat liver mitochondria. *J. Cell Biol.* 38:158–175.

37. Schneider, H., J. J. Lemasters, M. Hoechli, and C. R. Hackenbrock. 1980. Liposome-mitochondrial inner membrane fusion. Lateral diffusion of integral electron transfer components. *J. Biol. Chem.* 255:3748–3756.

38. Schwerzmann, K., and H. Hoppeler. 1985. Stereology: a working tool for cell biologists. *Trends Biochem. Sci.* 10:184–187.

39. Small, J. V. 1968. Measurements of section thickness. Proceedings of the 4th European Congress on Electron Microscopy. 1:609–610.

40. Srere, P. A. 1980. The infrastructure of the mitochondrial matrix. *Trends Biochem. Sci.* 5:120–121.

41. Takano, T., and R. E. Dickinson. 1980. Redox conformation changes in refined Tuna cytochrome c. *Proc. Natl. Acad. Sci. USA.* 77:6371–6375.

42. Vanderkooi, G. 1978. Organization of proteins and lipid components in Membranes. *In* Molecular Biology of Membranes. S. Fleischer, Y. Hatefi, D. MacLennan, and A. Tzagaloff, editors. Plenum Publishing Corp. New York. 25–55.

43. Weibel, E. R. 1979. Stereological Methods. Vol. I. Academic Press, London and New York.

44. Weibel, E. R. 1984. The Pathways for Oxygen. Harvard University Press, Cambridge (USA) and London.

45. Williams, J. N. 1984. A method for the simultaneous quantitative estimation of cytochromes a, b, c1 and c in mitochondria. *Arch. Biochem. Biophys.* 107:537–543.

46. Wrigglesworth, J. M., L. Packer. 1970. Organization of mitochondrial structure as revealed by freeze-fracture. *Biochim. Biophys. Acta.* 205:125–135.